research articles Journal of proteome research

Modeling Protein−Protein Complexes Involved in the Cytochrome *c* Oxidase Copper-Delivery Pathway

Aalt D. J. van Dijk,[†] Simone Ciofi-Baffoni,[‡] Lucia Banci,[‡] Ivano Bertini,[‡] Rolf Boelens,[†] and Alexandre M. J. J. Bonvin*[,†]

Bijvoet Center for Biomolecular Research, Science Faculty, Utrecht University, 3584CH, Utrecht, The Netherlands, and Magnetic Resonance Center CERM and Department of Chemistry, University of Florence, Via Luigi Sacconi 6, 50019, Sesto Fiorentino, Florence, Italy

Received December 6, 2006

Proper assembly and function of cytochrome *c* oxidase, which catalyzes the reduction of O_2 and generates the proton gradient driving ATP synthesis, depend on correct copper delivery and incorporation. Structural details about the protein−protein complexes involved in this process are still missing. We describe here models of four complexes along this pathway obtained by combining bioinformatics interface predictions with information-driven docking and discuss their relevance with respect to known and pathogenic mutations.

Keywords: Docking • cytochrome *c* oxidase • Cox17 • Sco1 • Cox11 • CoxII • interface prediction • copper delivery • HADDOCK

Introduction

The reduction of molecular oxygen, catalyzed by cytochrome *c* oxidase (CcO) (the terminal enzyme in the electron transport system) is of vital importance, since it generates the proton gradient that drives synthesis of ATP. Multiple subunits and several cofactors are necessary for catalytic activity, including two hemes, a magnesium ion, a zinc ion, and three copper ions. In particular, the copper ions are located in subunits CoxI and CoxII, which contain the Cu_B and Cu_A centers, respectively. CcO is located in the inner mitochondrial membrane, and the two copper binding subunits are encoded by the mitochondrial genome; therefore, copper insertion must occur within this organelle. Insertion of these cofactors and assembly of the CcO complex requires a number of accessory proteins,[1] but little is known about this assembly process.

In particular, the mechanism of copper delivery to CcO is a long-standing puzzle. In eukaryotes, copper insertion involves the key mitochondrial copper chaperone Cox17, which acts as a donor of Cu(I) to both Sco1 and Cox11.[2] Sco1 is known to interact with CoxII[3] and is proposed to donate Cu(I) to the Cu_A center, whereas Cox11 is a mitochondrial co-chaperone that provides copper to the Cu_B center of the subunit CoxI.[4] CoxII is an integral membrane subunit of CcO anchored to the inner membrane of mitochondria through two transmembrane helices. Its hydrophilic C-terminal part contains the copper binding site and projects out in the inner membrane space. Both Sco1 and Cox11 are anchored to the mitochondrial inner membrane by a single transmembrane helix with the soluble domain located in the inner membrane space, whereas Cox17 is a nonmembrane protein. A schematic overview of this pathway is shown in Figure 1. The importance of copper and the essential role of these proteins are indicated by the onset of various pathologies when the function of one of these proteins is impaired by protein mutation.[5−7] Although 3D structures of the individual proteins are known, nothing is known about their interaction mode, and full experimental characterization of the complexes is hampered, among others, by the instability of a number of components and the transient nature of the protein−protein interaction which does not therefore produce sizably populated states.[8]

Docking is a computational methodology that uses the known structures of the components of a complex to generate a model for the complex. Docking approaches are becoming increasingly popular for investigating intermolecular complexes whose structures cannot be studied by classical structural methods.[9−11] They have been applied to a variety of complexes, among which are a complex related to the pathway we investigate here, cytochrome *c*−cytochrome *c* oxidase,[12] and some other copper transfer complexes, such as $PacS_N$−ScAtx1[13] and Atx1−Ccc2.[14]

Here, we apply the data-driven docking approach HADDOCK[15] to model complexes along the CcO copper-delivery pathway for human proteins. Since no experimental information is available for the complexes that are formed (in contrast to the previously studied complexes mentioned above), we use bioinformatics tools to predict interface residues in order to generate restraints to drive the docking. Specifically, we model the interactions between Cox17 and Sco1, Sco1 and CoxII, Cox17 and Cox11, and Cox11 and Cox11 (since Cox11 is known to form a homodimer[16,17]). Note that we do not model the Cox11−CoxI complex, since the Cu_B site is buried deeply inside CoxI, and copper insertion is thought to occur co-translation-

* Corresponding author: Alexandre M. J. J. Bonvin. E-mail: a.m.j.j.bonvin@chem.uu.nl; tel., +31.(0)30.2532652; fax, +31.(0)30.2537623.
[†] Utrecht University.
[‡] University of Florence.

10.1021/pr060651f CCC: $37.00
Published on Web 03/06/2007

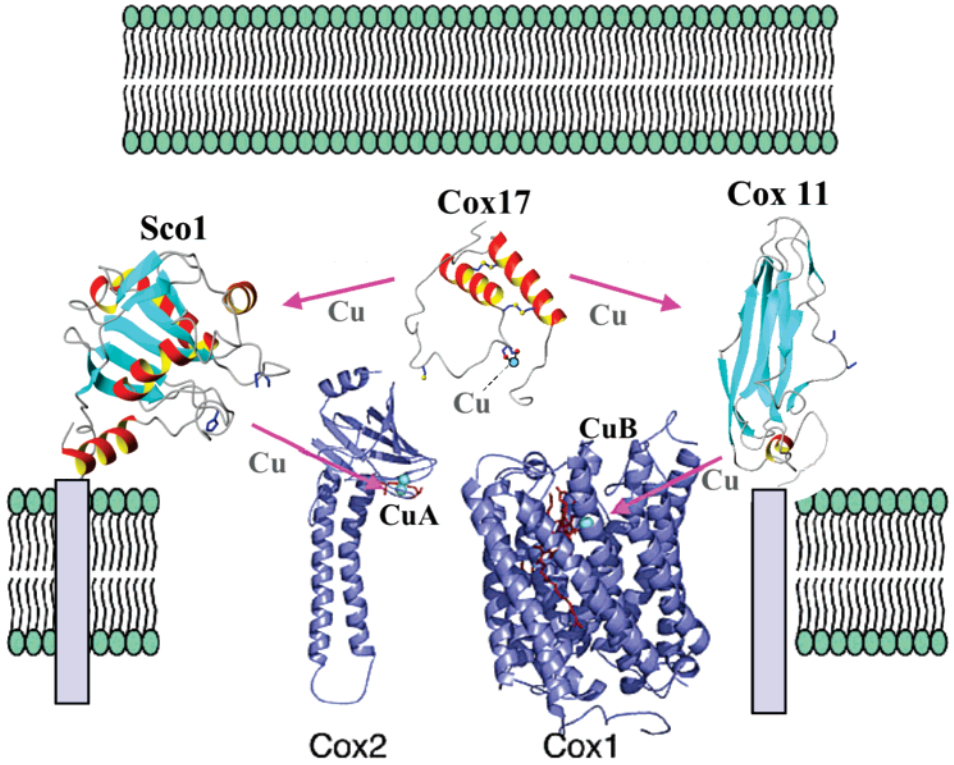

Figure 1. Overview of the copper metalation pathway of CoxI and CoxII mediated by Cox11 and Sco1, respectively. CoxI, CoxII, Cox11, and Sco1 are part of the mitochondrial inner membrane, whereas Cox17 is in the intermembrane space. Arrows indicate the transfer of copper. We modeled the interactions depicted in this figure: Cox17−Sco1, Sco1−CoxII, and Cox17−Cox11, and in addition, the Cox11 homodimer (see text for details); we did not model the Cox11−CoxI interaction, since copper is thought to be inserted in CoxI co-translationally before folding of CoxI.

ally, that is, before CoxI folding.[18,19] As we recognize the importance of metal ions in mediating protein−protein interactions in such systems,[20] all models are generated in the explicit presence of copper, making use, when available, of experimental information about its coordination derived from EXAFS data. A similar approach has been applied for the modeling of the Atx1−Ccc2 complex,[14] which structure was later confirmed experimentally,[20] thus, providing confidence in the modeling strategy followed here.

Methods

Structural Coordinates. Models for the human proteins along the copper-delivery pathway were generated with Modeller 6[41] using the templates listed in Table 1 of Supporting Information. Out of 1000 generated models, the 10 best based on the objective score were used for docking. WHATIF[42] was used for determination of the protonation state of the histidines. Copper was introduced with charge +1; for the appropriate cysteines (see Table 1), the SH atom was removed and the partial charges for side chain atoms were set to +0.18 for CB and −0.45 for SG (instead of −0.68). In this way, the total net charge of two cysteines plus copper is zero. All nonpolar hydrogens were removed to speed up the docking calculations.

Interface Prediction. WHISCY[22] and ProMate[23] were used for interface predictions and combined for consensus scoring using WHISCYMATE.[22] Multiple sequence alignments were constructed by first finding homologues of the human proteins using blastp against the nr database using default settings (Word Size 3; Expect 10; Blosum62 matrix; Gap Costs: existence 11, extension 1),[43] except that a restriction to only eukaryote sequences was used since the copper-delivery pathway might be different in prokaryotes as compared to eukaryotes (for example, Cox17 is only found in eukaryotes[44]). Subsequently, multiple sequence alignment was performed using ClustalW 1.83.[45] ProMate predictions were obtained making use of the Web interface of ProMate (http://bioportal.weizmann.ac.il/promate/), using default settings. For WHISCYMATE, a residue was predicted if its ProMate score was higher than or equal to 98.520, its WHISCY score higher than or equal to 0.371, or if its ProMate and WHISCY scores were both higher than or equal to 55.420 and 0.107, respectively. Interface predictions were used to generate Ambiguous Interaction Restraints as discussed before:[22] predicted residues were designated active residues and their surface neighbors passive residues. We also used PPI-Pred[46] for interface prediction; PPI-Pred output consists of a most likely binding site location and two other possible binding site. In each case, the PPI-Pred predictions were overlapping with the WHISCYMATE predictions, although the overlap did not always occur with the most likely PPI-Pred predicted binding site.

Copper-Based Restraints. When appropriate, we defined (unambiguous) restraints between the copper and the S atoms of coordinating cysteines on both the delivering (holo) and accepting (apo) protein partner. The restraint distance was 2.4 ± 0.1 Å; residues involved in those restraints are listed in Table 1. For the Cox11 homodimer, restraints were based on EXAFS data which indicate the presence of three sulfur atoms at 2.23 Å in the first coordination shell of the copper ion, and a second copper at 2.7 Å.[16]

Docking Protocol. HADDOCK[15] uses ambiguous interaction restraints (AIRs) defined from any available information about

Table 1. List of Active and Passive Interface Residues Used for Docking[a]

	Cox17
Active	C23, C24, A25, C26, P27, R33, D34, C36, I37, C55, M56, A58, L59, G60, F61
Passive	P19, L20, K21, E28, K30, K31, A32, A35, E39, K40, G41, E42, E43, H44, G46, H47, E50, K53, E54, R57, K62
Cu-binding	Cys23, Cys26
	Sco1
Active	G10, F38, T39, C41, P42, D43, C45, P46, L49, F72, I75, D76, Y88, F92, A110, R111, Y113, R114, Y116, Y117, S118, Y128, I129, V130, D131, T133, I134, Y137, G143, F145, Y148
Passive	L7, L8, S13, Y27, L28, G29, E47, E50, E78, T81, A84, N87, K90, E91, P94, R103, E104, D107, Q108, A112, P119, G120, P121, K122, D125, E126, D127, D142, E144, L146, N152
Cu-binding	Cys41,Cys45
	Cox11
Active	Q38, Q39, L51, F53, K83, I84, Q85, C86, F87, C88, E90, V100, D101, M102, P103, V104, F105
Passive	G2, K20, N24, A25, D26, V27, N34, R36, T40, E41, Y43, E48, T49, A50, T69, N71, F75, Q79, Q92, R93, E98, E99, D122, L123, S127, T129, F131
Cu-binding	Cys86, Cys88; Cu−Cu restraint
	CoxII
Active	Q103, T104, Y121, R134, D139, D158, V159, Q195, S197, I199, G201, A202, N203, S205
Passive	N119, P124, P125, L128, L133, N140, R141, Q157, L160, P166, K171, D173, P176, V191
Cu-binding	Cys196, Cys200

[a] For all complexes, ambiguous interaction restraints were defined using active and passive residues as listed in the table, based on WHISCYMATE predictions. Active residues are residues predicted to be involved in the interaction, and passive residues are their surface neighbors. In addition, copper-based restraints were defined as described in Methods using the residues listed in the table.

the interface. In our case, active residues were based on interface predictions, as mentioned above. The definition of AIRs has been described in detail before.[15] The docking protocol consists of three consecutive stages:[15]

(i) randomization of orientations followed by rigid body energy minimization (EM);

(ii) semi-flexible simulated annealing in torsion angle space (TAD-SA), which consists of (ii-a) a rigid body Molecular Dynamics search and first simulated annealing, (ii-b) a second semi-flexible simulated annealing during which side chains at the interface are free to move, and (ii-c) a third semi-flexible simulated annealing during which both side chains and backbone at the interface are free to move; and

(iii) final refinement in Cartesian space with explicit solvent.

The docking was performed starting from models for the human proteins along the Cu-delivery pathway (see above). For each protein, 10 models were used, resulting in 100 different combinations. In the initial rigid body docking phase, 1000 structures were generated (10 for each combination), and the best 200 in terms of total intermolecular energy were further submitted to the semi-flexible simulated annealing and final water refinement. Flexible segments were based on the active and passive residues ±2 consecutive residues. In addition, for Cox17, the first 22 disordered residues were treated as fully flexible.

Nonbonded intermolecular interactions were calculated with an 8.5 Å cutoff using the OPLS parameters.[47] The dielectric constant epsilon was set to 10 in the vacuum part of the protocol and to 1 for the explicit solvent refinement. To account for the presence of false positives in the interface predictions, for each docking trial, 50% of the restraints based on the interface predictions were randomly discarded. To keep the secondary structure elements intact during the simulated annealing refinement, hydrogen bond and dihedral angle restraints were introduced. We used DSSP[48] to identify secondary structure elements in the top ranking homology model: dihedral angle restraints were defined as the measured dihedral angle ± a 20° range, and in the case of α-helices, hydrogen bond restraints were defined between each O(i)−N(i+4) pair (lower and upper bound 2.3 and 3.5 Å, respectively) and O(i)−HN(i+4) pair (lower and upper bound 1.7 and 2.5 Å, respectively). In addition, we used $C2$-symmetry restraints[49] and NCS-restraints for the Cox11 homodimer.

The structures were ranked based on the HADDOCK score with standard weights[50] (after water refinement: HADDOCK score = 1.0·Evdw + 0.2·Eelec + 0.1·Edist 0.1 + 1.0·Esolv, where the four terms in the summation are the van der Waals energy, electrostatic energy, distance restraint energy, and desolvation energy terms, respectively). In addition, we also scored the solutions using DFIRE (a statistical energy function based on the reference state of distance-scaled, finite, ideal gases[51]), FastContact (an estimate of the binding free energy based on a statistically determined desolvation contact potential and Coulomb electrostatics with a distance-dependent dielectric constant[52]), and Probe (which uses small-probe contact dots to assess the goodness-of-fit[53]); the latter was calculated using the MolProbity package.[54] The final selection of clusters was based on the HADDOCK score.

The docking solutions were clustered based on positional rmsd values using a 7.5 Å cutoff; only clusters with at least 5 members were analyzed. The rmsd values were calculated on the interface backbone atoms of the smallest component after superposition on the interface backbone atoms of the largest component. This can be termed "ligand interface rmsd".

Analysis of Intermolecular Contacts. Intermolecular contacts (hydrogen bonds and nonbonded contacts) were analyzed with DIMPLOT, which is part of the LIGPLOT software,[55] using the default settings (3.9 Å heavy-atoms distance cutoff for nonbonded contacts; 2.7 and 3.35 Å proton−acceptor and donor−acceptor distance cutoffs, respectively, with minimum 90° angles (D−H−A, H−A−AA, D−A−AA) for hydrogen bonds. A contact is defined to be present if it is found in at least 3 of the 5 best structures.

Results and Discussion

Bioinformatic Prediction-Driven Modeling. To obtain insight into the CcO copper-delivery pathway, we modeled the structures of the human Cox17, Cox11, and CoxII (for details see Methods); the resulting structures, together with the recently solved structure of human Sco1[21] are shown in Figure 2, and some characteristics are listed in Table 1 of Supporting

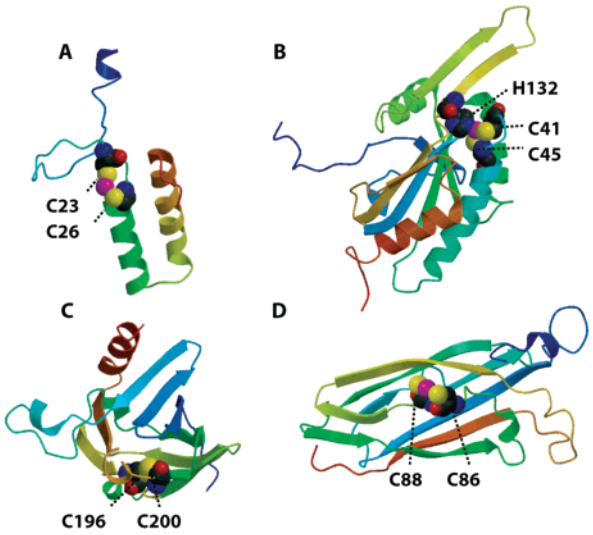

Figure 2. Ribbon representations of (A) the homology model of Cox17, (B) the NMR structure of Sco1, (C) the homology model of CoxII, and (D) the homology model of Cox11. The proteins are color coded using a color ramp from blue (N-term) to red (C-term). The copper coordinating residues are shown in cpk, and the copper atom is colored magenta (in Cox17, Sco1, and Cox11; CoxII is shown without copper since only apo-CoxII is used in the docking). Homology modeling was performed using Modeller as described in Methods using templates listed in Table 1 Supporting Information. The figures were generated using MolScript[56] and Raster3D.[57]

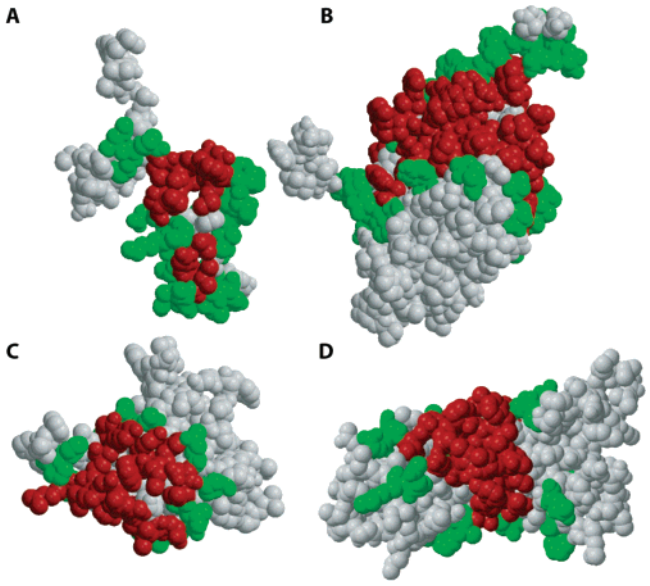

Figure 3. Space filling representation of the homology model of Cox17 (A), the NMR structure of Sco1 (B), and the homology models of CoxII (C) and Cox11 (D). Proteins are color coded to indicate active (red) and passive (green) residues used for docking (see Table 1 for the corresponding residue numbers). Active residues are defined based on interface predictions using WHISCY,[22] PROMATE,[23] and their combination WHISCYMATE;[22] passive residues are surface neighbors of active residues (see Methods).

Information. In Cox17 and Cox11, the copper ion was placed halfway between the S-atom of two coordinating cysteines (see Table 1), and the structure was subjected to a short energy minimization; the Sco1 structure already contained copper. These structures were used as input structures for modeling the following complexes: Cox17(Cu)−Sco1, Sco1(Cu)−CoxII, Cox17(Cu)−Cox11, and Cox11(Cu)−Cox11(Cu). Since there is no experimental information on the protein−protein interface in those complexes, we used WHISCY[22] and PROMATE[23] interface predictions (see Methods) to generate ambiguous interaction restraints (AIRs) to drive the docking. The predicted interaction surfaces are summarized in Table 1 and are also mapped onto the respective structures in Figure 3. In all cases, the predictions indicate patches around the copper-binding site, which makes sense, since these proteins interact in order to transfer copper. Note that we did not restrict the interaction region to this site; the fact that they do cluster around the copper binding sites makes us confident that those predictions are meaningful and can be used in the modeling of these complexes. In addition to the interface prediction-based restraints, we also defined restraints between the copper and each of the coordinating cysteines of both protein partners (for details see Methods). For each complex, we performed three different docking runs, using (i) the AIRs based on interface predictions, (ii) the copper-based restraints, and (iii) both restraints simultaneously. Similar results were obtained with the various approaches, but since the latter approach gave the best convergence, we will only present results from the docking runs using the combined set of restraints.

The calculated adduct structures were then clustered, based on their pairwise rmsd values, using a 7.5 Å cutoff. In Table 2, the statistics of the resulting clusters are shown, including rmsd from the lowest energy structure and scores according to different scoring schemes. The latter include HADDOCK score and DFIRE, FastContact, and Probe (see Methods). As a general rule, we propose as predicted model the structures with the lowest HADDOCK score from the cluster with the lowest average HADDOCK score. For Sco1−CoxII and Cox17−Cox11, this leads to the unambiguous selection of one cluster; for Cox17−Sco1 and Cox11−Cox11, however, there are two clusters with almost equal score (see further discussion below). The structural models for these four complexes are shown in Figure 4; Table 2 of Supporting Information summarizes the observed intermolecular contacts, and Supporting Information Table 3 gives statistics of copper−cysteine contacts in the models. In the following, we will analyze them in more detail and discuss their biological implications.

Analysis of Copper-Transfer Complexes. 1. Cox17−Sco1. As noted above, we find two clusters of solutions for the Cox17−Sco1 complex, with comparable HADDOCK score (although cluster 1 scores slightly better when assessed by FastContact, Dfire, and Probe, see Table 2). As shown in Figure 4, the orientation of the two molecules in these models is rather different. This is reflected in the difference between intermolecular contacts in the two clusters (see Table 2 Supporting Information). One key difference is the role of Cox17 Arg33, which is expected to be involved in complex formation with Sco1, as it results from mutagenesis studies.[24] In both clusters, it is involved in an intermolecular salt bridge, with Glu48 in cluster 1 and with Asp123 in cluster 2. Another difference is found for the interaction of Cox17 Phe61. In cluster 1, Phe61 is involved in contacts with Arg114, Ile135, and Tyr137, whereas in cluster 2, it contacts Asp43, Val44, and Glu47. These data provide testable hypotheses for mutation experiments in order to select between the two models.

We analyzed our models to gain some insight into the copper transfer mechanism. When the copper-based restraints are

Table 2. Statistics of Clusters Obtained by Data-Driven Docking[a]

no.[c]	N_{st}	rmsd -Emin	HADDOCK score	Dfire	BSA (Å^2)	Fastcontact (kcal/mol)	probe (a.u.)	d (Å)[b]
				Cox17 (Cu)−Sco1 (apo)				
1	**33**	**3.8 (2.0)**	**−140 (15)**	**−19.2 (1.9)**	**2289 (247)**	**−42.1 (3.1)**	**8.7 (6.4)**	**2.6**
2	**56**	**13.6 (0.6)**	**−135 (10)**	**−16.1 (1.8)**	**2412 (285)**	**−37.1 (4.4)**	**7.2 (8.9)**	**2.2**
3	27	9.3 (1.0)	−112 (12)	−16.5 (2.0)	2192 (254)	−25.6 (6.7)	−0.8 (9.0)	2.2
4	9	13.6 (0.4)	−106 (44)	−19.6 (2.3)	2354 (388)	−38.8 (8.7)	17.6 (14.2)	2.2
5	24	10.7 (2.0)	−95 (17)	−14.7 (1.8)	1962 (238)	−43.0 (5.7)	14.3 (9.3)	2.2
6	15	5.9 (1.4)	−93 (22)	−16.6 (3.1)	2031 (284)	−41.6 (7.4)	14.3 (11.8)	2.3
7	8	9.2 (1.7)	−74 (7)	−15.6 (2.2)	1887 (220)	−37.2 (8.8)	12.3 (6.4)	2.2
				Sco1 (Cu)−CoxII (apo)				
1	**132**	**6.5 (3.3)**	**−106 (5)**	**−18.2 (1.3)**	**1943 (181)**	**−25.1 (6.1)**	**11.5 (8.1)**	**2.5**
2	12	13.9 (0.6)	−86 (6)	−18.3 (1.0)	1938 (76)	−26.5 (3.8)	11.9 (4.6)	16.5
3	14	14.0 (2.2)	−65 (5)	−14.7 (0.5)	1798 (194)	−17.3 (3.0)	20.2 (5.3)	5.7
4	9	11.2 (0.7)	−45 (17)	−14.0 (1.3)	1691 (219)	−22.1 (2.7)	7.4 (10.7)	4.0
5	8	16.5 (1.1)	−44 (8)	−14.4 (0.7)	1685 (237)	−19.0 (4.7)	9.1 (9.8)	8.1
6	7	9.4 (1.2)	−34 (9)	−15.2 (1.4)	1858 (214)	−15.2 (4.1)	9.5 (4.7)	11.4
				Cox17 (Cu)−Cox11 (apo)				
1	**125**	**4.5 (2.9)**	**−159 (8)**	**−17.8 (0.6)**	**1835 (134)**	**−39.6 (5.9)**	**6.8 (5.2)**	**2.1**
2	15	6.1 (1.7)	−148 (6)	−17.6 (0.9)	1998 (158)	−39.3 (5.4)	11.6 (8.3)	2.1
3	26	8.9 (1.4)	−137 (7)	−18.0 (0.6)	1885 (162)	−36.8 (6.2)	17.5 (11.3)	2.1
4	12	14.4 (1.2)	−113 (9)	−15.0 (1.6)	1779 (129)	−29.7 (6.6)	3.0 (7.5)	2.1
5	10	8.0 (1.9)	−112 (11)	−14.4 (1.0)	1828 (119)	−26.1 (7.1)	10.8 (12.6)	2.1
				Cox11 (Cu)−Cox11 (Cu)				
1	**40**	**1.8 (1.2)**	**−117 (8)**	**−18.8 (1.0)**	**2291 (135)**	**−30.2 (2.3)**	**4.1 (6.2)**	**-**
2	**22**	**8.2 (0.3)**	**−117 (6)**	**−19.5 (2.0)**	**2366 (114)**	**−30.7 (3.0)**	**7.2 (6.8)**	**-**
3	114	16.9 (0.8)	−99 (6)	−16.4 (1.1)	1733 (98)	−19.8 (5.9)	1.8 (9.4)	-
4	8	20.7 (0.5)	−62 (6)	−16.9 (1.2)	1563 (112)	−12.1 (2.6)	−3.1 (15.7)	-

[a] Statistics of all clusters with at least 5 structures for the different docking runs. Averages (standard deviation in parentheses) were calculated over the best 5 structures of each cluster. N_{str}, number of structures in cluster (out of 200 water refined structures); score, HADDOCK score, defined as a weighted sum of different terms (see Methods); Dfire, statistical energy function based on the reference state of distance-scaled, finite, ideal gases;[51] BSA, buried surface area. **Bold** designates clusters selected as 'best', based on the HADDOCK score. [b] Lowest distance in best 5 structures from cluster between copper and Cys SG in Cu-accepting protein. [c] Cluster rank according to the HADDOCK score; as discussed in the text, for Cox17−Sco1 and Cox11−Cox11, two clusters were obtained that scored almost equally. These are referred to in the text as cluster 1 and cluster 2, respectively.

used in the calculation, in cluster 1, we find that the copper is preferably attaching to Sco1 Cys41 (the average copper−Cys41 distance is lower than the average copper−Cys45 distance, see Table 3A Supporting Information); in cluster 2, there is no difference between Cys41 and Cys45 in this respect. For the copper coordinating His132 in Sco1, we find in cluster 1 that this histidine is the last residue to enter the coordination sphere of copper; the average distance between NE2 of His132 and the copper is 4.9 ± 0.9 Å. For cluster 2, this histidine is, however, much closer to copper, with an average distance of 2.4 ± 0.8 Å.

Rerunning the water-refinement of the original docking run without any intermolecular copper-based restraints results in similar clusters, but now cluster 1 clearly scores better than cluster 2: the average HADDOCK score (standard deviation) is −154.6 (14.6) for cluster 1 compared with −126.6 (6.4) for cluster 2. Note that this is consistent with the differences in score according to FastContact, Dfire, and Probe, as mentioned above, indicating indeed a preference for cluster 1. Without the intermolecular copper-based restraints, the copper is not transferred to Sco1 in most structures, but in those where it is, again Cys41 is the accepting cysteine. In a docking run in which the copper restraints were not applied (data not shown), we also find that copper is accepted by Cys41 (in those complexes of the cluster where the transfer does occur).

2. Sco1−CoxII. The Cu_A site in CoxII contains a binuclear copper site, where the two copper ions are coordinated by two His, one Met, a backbone CO, and by two bridging Cys. The assembly mechanism of the binuclear center is not known; in this system, we modeled the transfer of one copper ion, assuming a mechanism of sequential insertion of the two copper ions (note that for modeling the transfer of the second copper the structure of CoxII−Cu_1 should be known). Sequential insertion is a reasonable model, as it is consistent with kinetic and copper binding studies on a Cu_A center engineered into *Pseudomonas aeruginosa* azurin, which showed the formation first of a Cu(I) monoderivative and then, after the following addition of Cu(II), the conversion of intermediate into the final purple Cu_A center.[25,26]

The copper center in CoxII is buried below the surface of the protein, and the coordinating cysteines have a relative low solvent accessibility in the starting models (7 ± 0.3% and 4 ± 1% for Cys196 and Cys200, respectively, as calculated over the ensemble of starting structures using NACCESS[27]). However, in many docking solutions, Cys200 becomes more solvent-exposed; in the 5 best structures of the selected cluster, the accessibility of Cys196 is still low, 2 ± 1%, while that of Cys200 has now increased to 33 ± 19%. On the basis of our docking results, we predict that Cys200 is the cysteine that first binds the copper ion upon interaction with Sco1. In some models, the copper ion is still close to one of the starting cysteines (either Cys41 or Cys45) of Sco1, and in others, it is transferred to CoxII Cys200. In the latter case, Sco1 His132 is no longer coordinating the copper ion. The fact that His132 is the first residue to leave the coordination sphere of the copper is in agreement with the behavior of cluster 1 of the Cox17−Sco1 docking, where, upon transfer of copper toward Sco1, His132 was the last residue to accept the copper. The behavior of His being the weaker ligand to copper has been observed also for other complexes of copper transporting proteins, such as the $PacS_N$−Atx1 complex,[13] where Atx1 His 61 is the first to be displaced from coordination once the complex is formed.

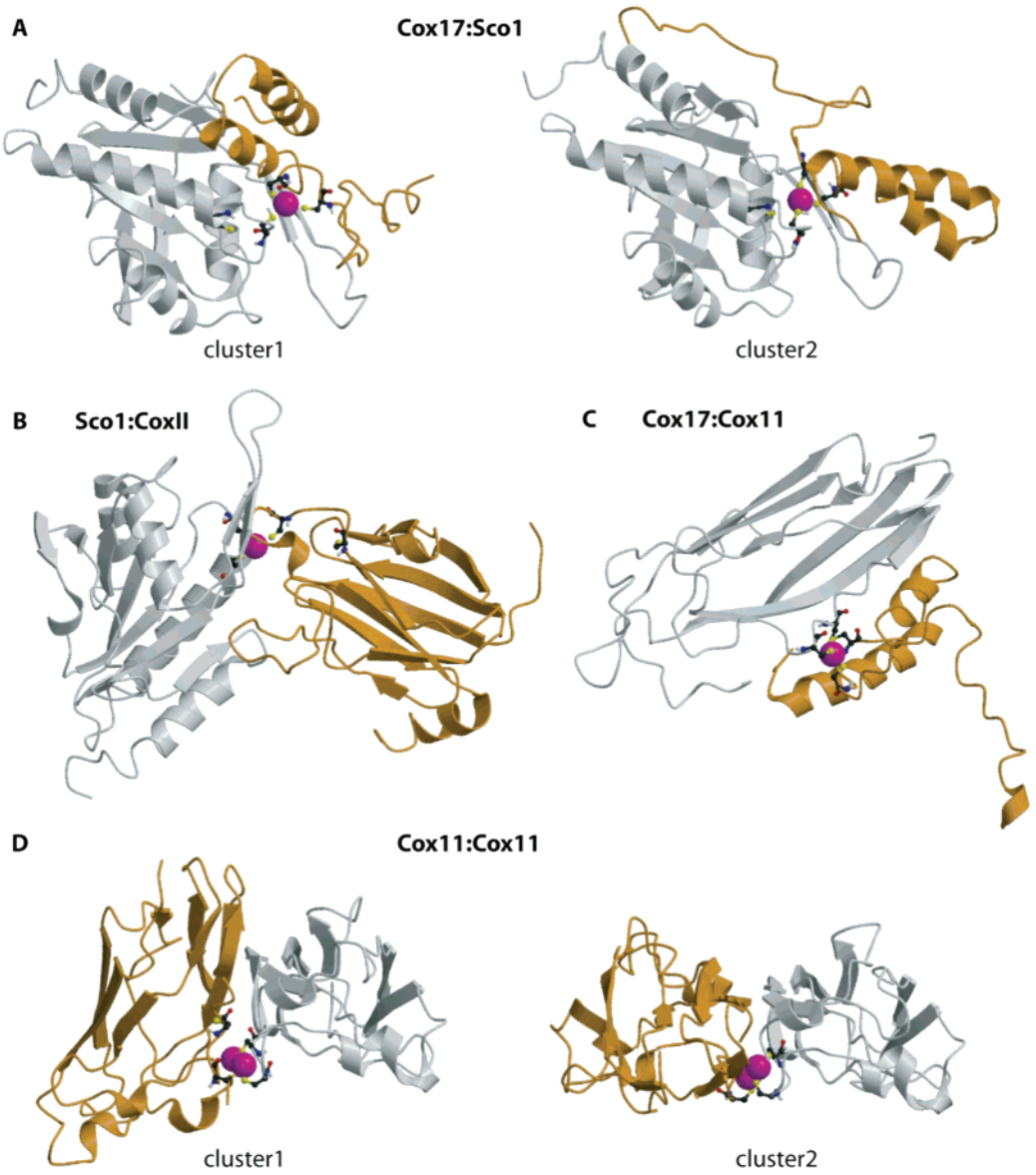

Figure 4. HADDOCK models of the complexes along the human cytochrome *c* oxidase copper-delivery pathway: (A) Cox17−Sco1, (B) Sco1−CoxII, (C) Cox17−Cox11, and (D) Cox11−Cox11. Color coding: Cox17 (A and C) in orange; CoxII (B) in orange; Sco1 (A and B) and Cox11 (C) in white. In panel D, one of the Cox11 monomers is orange and the other monomer is white. Note that for Cox17−Sco1 and Cox11−Cox11, as discussed in the text, there are two clusters of solutions with identical scores.

The distance copper travels from one protein to another can be assessed by fitting both the CoxII and the Sco1 starting structure onto the modeled complex and calculating the distances between the copper in the docking model and the copper in the initial Sco1 and CoxII structures. For the best five structures of the cluster, the first distance is either 1−2 Å, which is comparable to the precision of the cluster, indicating that copper essentially remains bound to Sco1, or is around 5 Å, in the two cases where copper is transferred to CoxII Cys200. In the latter case, the copper ion is approximately halfway the path it has to travel from the Sco1 to the CoxII site, which is approximately 11 Å. Because of the burial of the copper site in CoxII, this distance is rather large, and our model most likely only represents an intermediate state of the copper transfer.

3. Cox17−Cox11. As the structure of dimeric Cox11 is not yet available (see below for our docking model for this dimer), and as the monomeric Cox11−Cox17 complex is likely to be an intermediate for copper transfer from Cox17 to Cox11, we modeled the latter complex.

It has been suggested previously that Glu90 and Glu91 in Cox11, which are conserved in eukaryotes but not in prokaryotes, could be involved in complex formation with Cox17[16] (note that Cox17 is not present in prokaryotes). In the selected structures, Glu91 does not form any intermolecular contacts; in fact, in the starting structure, it forms two intramolecular hydrogen bonds *via* its two OE atoms to two backbone amides. This intramolecular role is further supported by the fact that in prokaryotes Glu91, although not fully conserved, is in fact present more often than Glu90. In contrast, Glu90 is found to be involved in contacts with Cox17; these are however not well-defined, since various salt bridges to lysines of Cox17 are observed (Lys21, Lys30, and Lys31). Over the whole cluster, however, there is a clear preference for Glu90 of Cox11 to form

contacts with Lys30 and Lys31 of Cox17 (almost 50% of the 125 structures have Glu90 salt-bridged with both Lys30 and Lys31).

With respect to the copper transfer pathway, we find that copper first detaches from Cys26 of Cox17, since in 83 structures out of 125, the copper is close to Cys23 (2.2 ± 0.1 Å) and far from Cys26 (5.2 ± 2.1 Å); in the other 42 structures, the copper is still bound to both Cys23 and Cys26. On the Cox11 side, the Cu ion is, in most cases, bound to both Cys86 and Cys88 (107 out of 125 structures in the top ranking cluster have the Cu within 3 Å of both cysteines), indicating that copper transfer in this case has almost fully occurred. This means that our model for the Cox17−Cox11 complex represents a state in the transfer pathway closer to the final copper-loaded Cox11 as compared to the Cox17−Sco1 complex. This obviously has to do with the fact that the two accepting Cys on Cox11 are more easily accessible; the relative accessibilities of Cys86 and Cys88 in Cox11 (calculated using NACCESS over the ensemble of starting structures) are 55 ± 10% and 32 ± 9%, respectively, whereas these are only 16 ± 7% and 3 ± 3% for Cys41 and Cys45 in Sco1.

4. Cox11−Cox11. The dimerization of Cox11 has been shown to occur in bacteria and yeast upon Cu(I) binding forming a binuclear Cu(I) thiolate cluster at the dimer interface.[16,17] In addition, size exclusion chromatography followed by immunoblot analysis of human Cox11 isolated from mitochondria showed that it exist as a homodimer.[28]

In this case, docking results in two clusters with comparable scores (both HADDOCK as well as other scores, see Table 2). The two clusters have a somewhat different orientation, but involve in both cases a hydrophobic interface consisting of Met102, Pro103, and Phe105. Both clusters reasonably fit the EXAFS data that were used as restraints, although cluster 2 shows a somewhat better agreement.

Interestingly, in both clusters, the two Cox11 molecules are oriented in an antiparallel arrangement; the angle between the two long molecular axes is between 20° and 40° in cluster 1 and between 10° and 15° in cluster 2. Taking into account that the N-terminal extension of Cox11 is attached to a transmembrane helix, this orientation means that the two copper ions and their surrounding face the membrane, as shown in Figure 5. It is thought that copper is inserted into CoxI co-translationally.[18] On the basis of our model, we speculate that copper could be brought into the membrane by virtue of the Cox11 homodimer inserting into the membrane. Indeed, Phe87 and Phe89, and Phe81 and Phe106, which are all conserved in eukaryotes, form a hydrophobic patch around the two copper ions (see Figure 5) that might promote interaction with the membrane. In this way, Cox11 dimerization could help in delivering Cu to CoxI. This is further supported by the fact that predicting membrane interaction surfaces for the dimer (as performed before for the monomer structures; see Methods) indicates a putative binding site at the membrane facing site around the copper involving the above-mentioned Phe residues.

Alternatively, this region might be involved in an interaction with another protein. The observation that Cox11 from *Schizosaccharomyces pombe* exists as a fusion protein with a protein homologous to *Saccharomyces cerevisiae* Rsm22 suggests that Cox11 may have an interaction with Rsm22. Rsm22 has indeed been proposed to have a role in mitochondrial translation.[18] The interaction between Cox11 and Rsm22 might, however, be indirect.[19]

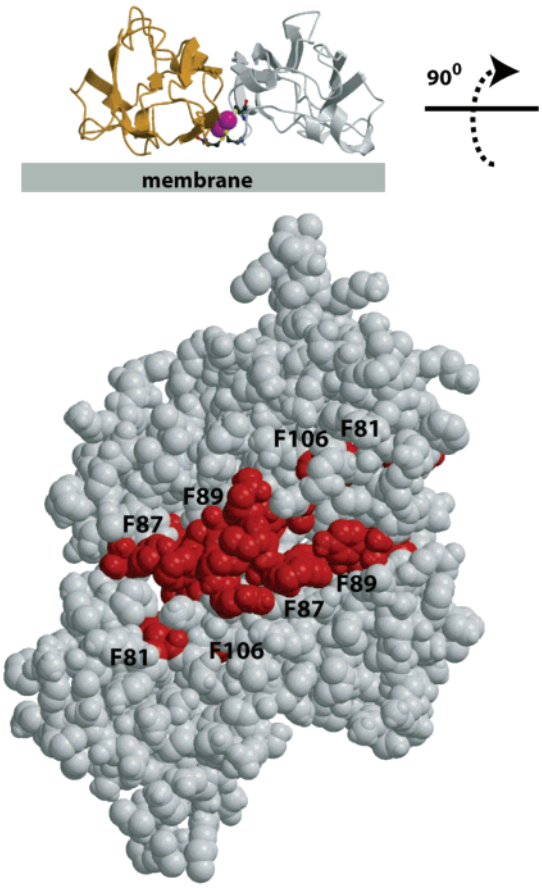

Figure 5. Resulting model for the Cox11−Cox11 homodimer as seen from the membrane side. Note that, as discussed in the text, there are two clusters of solutions with related but somewhat different orientations; here, we show the best scoring model from cluster 2. On the basis of our docking model, we predict that the dimer contains a protein or membrane interaction site; the residues in the dimer predicted by WHISCYMATE to form the interaction site are shown in red, and possibly interacting phenylalanines are indicated (see text for details).

Between the C-terminal hydrophilic domain and the transmembrane domain of Cox11, there is an unstructured linker of about 15 residues, containing a fully conserved cysteine necessary for growth on glycerol (alanine substitutions at these positions failed to restore growth on glycerol medium);[17] it was argued that in the dimer, this cysteine would be involved in an intermolecular disulfide bond with the corresponding cysteine of the other unit.[16] In both resulting clusters, the distance between the N-terminal residues of both monomers is around 25−30 Å, a distance which can be easily bridged by two stretches of 10−15 residues. This means that our structures are consistent with this model.

Relation to Human Diseases and Known Mutations. Cytochrome *c* oxidase deficiency is among the most frequent cases of respiratory chain defects in humans. A wide variety of clinical phenotypes can be present, primarily affecting those organs with high-energy demands such as brain, skeletal muscles, and heart.[29] Here, we discuss current knowledge on mutations in the cytochrome *c* oxidase copper-delivery proteins (some of which are disease-related) in the framework of our docking results.

It has been demonstrated that up-regulation of Cox17 is a frequent feature of non-small cell lung cancers,[30] and it was

speculated that there could be a possibility of designing anticancer drugs that target Cox17. If this would be a viable strategy, the structures of the complexes of Cox17 (Cox17−Sco1 and Cox17−Cox11) presented here are highly relevant, since one way to design such a drug would be via targeting one of those Cox17 complexes.

A study of *Cox17* mutants[24] highlighted the importance of Arg33 and Asp34, which, along with most of the Cys residues, appeared to be the only conserved residues affected by nonconservative replacements. Introduction of an oppositely charged residue at one of those positions resulted in a complete respiration deficiency, suggesting that the juxtaposition of two opposite charges at this location is critical for Cox17 function. Interestingly, in our docking results, we find that Arg33 interacts with Sco1 (in both clusters of solutions) but not with Cox11. This is perfectly consistent with the fact that Arg33 mutants show specifically an extensive loss of CoxII (to which copper would be directed via Sco1) and not of CoxI (to which copper would be directed via Cox11).[24]

The residues contacting Arg33 on Sco1 are Glu48 in cluster 1 and Asp123 in cluster 2 (see Table 2 Supporting Information). Especially the former possibility is highly interesting, since Glu48 in Sco1 corresponds to Glu140 in the Sco1-homologue Sco2; Glu140 is involved in the lethal mutation E140K in Sco2.[31,32] This means that if this model (cluster 1) is correct and also applies to Sco2, our Sco1−Cox17 model would suggest that a possible Sco2−Cox17 interaction would be disrupted by the E140K mutation which prevents the formation of the Arg33−Glu48 salt bridge. It is reasonable to hypothesize that Sco1 and Sco2 form similar complexes with Cox17, since their sequence identity is high, and all Sco1 residues contacting Cox17 in cluster1 are conserved in Sco2. Note that, as discussed above, cluster 1 seems somewhat more likely based on our scoring scheme. However, a mutation in Sco1 corresponding to the E140K mutation in Sco2 has not (yet) been found in patients.

The only known missense mutation in human Sco1, P174L, is associated with a fatal neonatal hepatopathy.[7] The molecular basis for dysfunction of the protein is unknown; two hypotheses are that either Pro174 is part of an interaction surface,[33] or the P174L mutation alters Sco1 chemical and structural properties. Our results show no involvement of Pro174 in the interaction with either Cox17 or CoxII, and consequently, we suggest that the latter hypothesis is correct. This also matches with the recent findings showing that the P174L mutant has an affinity for copper(I) which is lower than that of the wild-type protein.[8]

Finally, for Cox11, a set of mutants has been recently generated.[34] Since these experiments were performed before knowledge of the Cox11 3D structure, many of these are not very informative with respect to possible interaction surfaces (e.g., residues Asn58, Met118, Leu126, and Tyr128 are buried). Of the remaining mutations with considerable effect, Tyr70, Val104, and Asp109 are not involved in contacts in our docking solutions, whereas Pro103 is. In fact, Pro103 forms contacts both in the Cox11 homodimer and in the Cox11−Cox17 complex. Tyr70 and Val104 are part of a pocket in Cox11 with yet unknown function; these mutations may simply block this pocket.[34] The fact that we do not see contacts involving those residues is consistent with this idea. In addition, Tyr70 and Asp109 are located at the above-proposed putative membrane or Rsm22 interacting site, which might also explain the loss of function upon their mutation.

In an older study,[17] Cys and Met residues in Cox11 were mutated to elucidate which ones bind copper. Out of two conserved Met, Met102 and Met118 (their numbering: Met224 and Met240), only the mutation M224L led to a decrease in copper binding. On the basis of the structure of Cox11, it is clear that Met102 is not involved directly in contacts with copper. However, in cluster 1 of the Cox11−Cox11 docking solution, Met102−Met102 make tight inter-monomer contacts. Thus, the M224L mutation discussed above might interfere with dimer formation.

Computational Aspects. The selection of correct solutions (scoring) is a difficult problem in docking. In the present case, the fact that we know that the copper ion should be transferred imposes some additional restraints on the solutions, and this reduces the search space. For the Cox11 homodimer, we could, in addition, use EXAFS data. We validated our docking approach by repeating the docking of the Cox11 homodimer without the EXAFS-derived restraints. The clusters obtained in this way are similar to the ones obtained with inclusion of the EXAFS data (data not shown), which supports our docking approach.

It is interesting to analyze the influence of the starting structure used in the ensemble docking on the final result. For Sco1−CoxII and Cox17−Sco1, we find that whether the Cu ion is transferred toward the accepting partner depends on the specific starting structure used for the docking. For the Sco1−CoxII complex, the Sco1 starting models all have somewhat varying orientations for the long loop 8 (G120−I129), but there is no clear reason why some orientations would facilitate the transfer. What can be seen is that, when transfer takes place, Phe38, Val44, His132, and Ile134 show a somewhat different arrangement with respect to the starting structures; it is, however, not clear why this arrangement should be favorable (note that His132 is involved in the coordination of Cu). We also find for the Cox17−Cox11 complex a large influence of the starting conformation. As mentioned above, in this complex, the transfer is rather efficient. We observe that those models in which no transfer takes place are mostly derived from one specific starting conformation of Cox11 (i.e., the accepting partner in this case); in this particular structure, the two cysteines are somewhat further away from each other.

These observations all indicate that performing docking from ensembles of starting conformations is worthwhile, since it increases the chance of obtaining relevant conformations even at the price of a larger interaction space to be searched. This is in line with previous studies.[35−40]

The approach we used in this work, which is based on docking calculations, has been shown to be quite powerful in providing information on the interaction mode and on the functional steps of the copper transfer processes. This approach is the only way to structurally characterize transient, unstable complexes, when these are present only in low ratio with respect to the free proteins, thus, making their direct characterization by classical methods essentially impossible.

Conclusions and Perspectives

We modeled several complexes of human proteins involved in copper delivery to cytochrome *c* oxidase: Cox17−Sco1, Sco1−CoxII, Cox17−Cox11, and Cox11−Cox11. Details of these interactions have not been obtained before, due to experimental difficulties in obtaining the 3D structures of these complexes. Our models provide new information such as structural details on the mechanism of copper transfer in Cox17−Sco1,

Sco1−CoxII, and Cox17−Cox11. In addition, the Cox11−Cox11 homodimer suggests a possible membrane or protein interaction site, which might be involved in copper delivery to CoxI. Our models also provide testable hypotheses for mutagenesis experiments by suggesting structurally important residues, some of which are currently being mutated.

Finally, they provide a framework for understanding and rationalizing the known information about disease-related mutations in the cytochrome *c* oxidase copper-delivery pathway proteins. Our results on a limited pathway demonstrate the viability of data-driven docking and open the route to the modeling of larger pathways.

Acknowledgment. This work has been performed under the Project HPC-EUROPA (RII3-CT-2003-506079), with the support of the European Community, Research Infrastructure Action, under the FP6 "Structuring the European Research Area" Programme and was also supported by the FP6 EU-NMR (contract 026145) and SPINE 2 (contract 031220) projects and by a "Jonge Chemici" grant (grant number 700.50.512) from The Netherlands Organization for Scientific Research (N.W.O.) to A.M.J.J.B.

Supporting Information Available: A PDF file containing three supplementary tables providing information on structures used for modeling, statistics of intermolecular contacts of the various complexes. and statistics of copper−cystein distances; six text files containing the coordinates of the complexes shown in Figure 4 (top 5 structures of each cluster) in PDB format. This material is available free of charge via the Internet at http://pubs.acs.org.

References

(1) Carr, H. S.; Winge, D. R. Assembly of cytochrome c oxidase within the mitochondrion. *Acc. Chem. Res.* **2003**, *36* (5), 309−316.
(2) Cobine, P. A.; Pierrel, F.; Winge, D. R. Copper trafficking to the mitochondrion and assembly of copper metalloenzymes. *Biochim. Biophys. Acta* **2006**, *1763* (7), 759−772.
(3) Lode, A.; Kuschel, M.; Paret, C.; Rodel, G. Mitochondrial copper metabolism in yeast: interaction between Sco1p and Cox2p. *FEBS Lett.* **2000**, *485* (1), 19−24.
(4) Hiser, L.; Di Valentin, M.; Hamer, A. G.; Hosler, J. P. Cox11p is required for stable formation of the Cu-B and magnesium centers of cytochrome c oxidase. *J. Biol. Chem.* **2000**, *275* (1), 619−623.
(5) Papadopoulou, L. C.; Sue, C. M.; Davidson, M. M.; Tanji, K.; Nishino, I.; Sadlock, J. E.; Krishna, S.; Walker, W.; Selby, J.; Glerum, D. M.; Van Coster, R.; Lyon, G.; Scalais, E.; Lebel, R.; Kaplan, P.; Shanske, S.; De Vivo, D. C.; Bonilla, E.; Hirano, M.; DiMauro, S.; Schon, E. A. Fatal infantile cardioencephalomyopathy with COX deficiency and mutations in SCO2, a COX assembly gene. *Nat. Genet.* **1999**, *23* (3), 333−337.
(6) Sue, C. M.; Karadimas, C.; Checcarelli, N.; Tanji, K.; Papadopoulou, L. C.; Pallotti, F.; Guo, F. L.; Shanske, S.; Hirano, M.; De Vivo, D. C.; Van Coster, R.; Kaplan, P.; Bonilla, E.; DiMauro, S. Differential features of patients with mutations in two COX assembly genes, SURF-1 and SCO2. *Ann. Neurol.* **2000**, *47* (5), 589−595.
(7) Valnot, I.; Osmond, S.; Gigarel, N.; Mehaye, B.; Amiel, J.; Cormier-Daire, V.; Munnich, A.; Bonnefont, J. P.; Rustin, P.; Rotig, A. Mutations of the SCO1 gene in mitochondrial cytochrome c oxidase deficiency with neonatal-onset hepatic failure and encephalopathy. *Am. J. Hum. Genet.* **2000**, *67* (5), 1104−1109.
(8) Banci, L.; Bertini, I.; Ciofi-Baffoni, S.; Leontari, I.; Martinelli, M.; Palumaa, P.; Sillard, R.; Wang, S. Human Sco1 functional studies and pathological implications of P174L mutant. *Proc. Natl. Acad. Sci. U.S.A.* **2007**, *104* 15−20.
(9) van Dijk, A. D. J.; Boelens, R.; Bonvin, A. M. J. J. Data-driven, docking for the study of biomolecular complexes. *FEBS J.* **2005**, *272* (2), 293−312.
(10) Bonvin, A. M. Flexible protein-protein docking. *Curr. Opin. Struct. Biol.* **2006**, *16* (2), 194−200.
(11) Gray, J. J. High-resolution protein-protein docking. *Curr. Opin. Struct. Biol.* **2006**, *16* (2), 183−193.
(12) Bertini, I.; Cavallaro, G.; Rosato, A. A structural model for the adduct between cytochrome c and cytochrome c oxidase. *J. Biol. Inorg. Chem.* **2005**, *10* (6), 613−624.
(13) Banci, L.; Bertini, I.; Ciofi-Baffoni, S.; Kandias, N. G.; Robinson, N. J.; Spyroulias, G. A.; Su, X. C.; Tottey, S.; Vanarotti, M. The delivery of copper for thylakoid import observed by NMR. *Proc. Natl. Acad. Sci. U.S.A.* **2006**, *103* (22), 8320−8325.
(14) Arnesano, F.; Banci, L.; Bertini, I.; Bonvin, A. M. J. J. A docking approach to the study of copper trafficking proteins: Interaction, between metallochaperones and soluble domains of copper ATPases. *Structure* **2004**, *12* (4), 669−676.
(15) Dominguez, C.; Boelens, R.; Bonvin, A. M. J. J. HADDOCK: A protein-protein docking approach based on biochemical or biophysical information. *J. Am. Chem. Soc.* **2003**, *125* (7), 1731−1737.
(16) Banci, L.; Bertini, I.; Cantini, F.; Ciofi-Baffoni, S.; Gonnelli, L.; Mangani, S. Solution, structure of Cox11, a novel type of beta-immunoglobulin-like fold involved in Cu-B site formation of cytochrome C oxidase. *J. Biol. Chem.* **2004**, *279* (33), 34833−34839.
(17) Carr, H. S.; George, G. N.; Winge, D. R. Yeast Cox11, a protein essential for cytochrome c oxidase assembly, is a Cu(I)-binding protein. *J. Biol. Chem.* **2002**, *277* (34), 31237−31242.
(18) Carr, H. S.; Maxfield, A. B.; Horng, Y. C.; Winge, D. R. Functional analysis of the domains in Cox11. *J. Biol. Chem.* **2005**, *280* (24), 22664−22669.
(19) Khalimonchuk, O.; Ostermann, K.; Rodel, G. Evidence for the association of yeast mitochondrial ribosomes with Cox11p, a protein required for the Cu-B site formation of cytochrome c oxidase. *Curr. Genet.* **2005**, *47* (4), 223−233.
(20) Banci, L.; Bertini, I.; Cantini, F.; Felli, I. C.; Gonnelli, L.; Hadjiliadis, N.; Pierattelli, R.; Rosato, A.; Voulgaris, P. The Atx1-Ccc2 complex is a metal-mediated protein-protein interaction. *Nat. Chem. Biol.* **2006**, *2* (7), 367−368.
(21) Banci, L.; Bertini, I.; Calderone, V.; Ciofi-Baffoni, S.; Mangani, S.; Martinelli, M.; Palumaa, P.; Wang, S. A hint for the function of human Sco1 from different structures. *Proc. Natl. Acad. Sci. U.S.A.* **2006**, *103* (23), 8595−8600.
(22) de Vries, S. J.; van Dijk, A. D. J.; Bonvin, A. M. J. J. WHISCY: What information does surface conservation yield? Application to data-driven docking. *Proteins: Struct., Funct., Bioinf.* **2006**, *63* (3), 479−489.
(23) Neuvirth, H.; Raz, R.; Schreiber, G. ProMate: A structure based prediction program to identify the location of protein-protein binding sites. *J. Mol. Biol.* **2004**, *338* (1), 181−199.
(24) Punter, F. A.; Glerum, D. M. Mutagenesis reveals a specific role for Cox17p in copper transport to cytochrome oxidase. *J. Biol. Chem.* **2003**, *278* (33), 30875−30880.
(25) Hay, M. T.; Lu, Y. Metal-binding properties of an engineered purple CuA center in azurin. *J. Biol. Inorg. Chem.* **2000**, *5* (6), 699−712.
(26) Wang, X. T.; Ang, M. C.; Berry, S. M.; Lu, Y. Kinetic of copper incorporation into an engineered purple Cu-A azurin. *Abstr. Pap.—Am. Chem. Soc.* **1999**, *217,* U1062−U1062.
(27) Hubbard, S. J.; Thornton, J. M., *NACCESS*. Department of Biochemistry and Molecular Biology, University College: London, 1993.
(28) Leary, S. C.; Kaufman, B. A.; Pellecchia, G.; Guercin, G. H.; Mattman, A.; Jaksch, M.; Shoubridge, E. A. Human SCO1 and SCO2 have independent, cooperative functions in copper delivery to cytochrome c oxidase. *Hum. Mol. Genet.* **2004**, *13* (17), 1839−1848.
(29) Shoubridge, E. A. Cytochrome c oxidase deficiency. *Am. J. Med. Genet.* **2001**, *106* (1), 46−52.
(30) Suzuki, C.; Daigo, Y.; Kikuchi, T.; Katagiri, T.; Nakamura, Y. Identification, of COX17 as a therapeutic target for non-small cell lung cancer. *Cancer Res.* **2003**, *63* (21), 7038−7041.
(31) Jaksch, M.; Ogilvie, I.; Yao, J. B.; Kortenhaus, G.; Bresser, H. G.; Gerbitz, K. D.; Shoubridge, E. A. Mutations in SCO2 are associated with a distinct form of hypertrophic cardiomyopathy and cytochrome c oxidase deficiency. *Hum. Mol. Genet.* **2000**, *9* (5), 795−801.
(32) Tay, S. K. H.; Shanske, S.; Kaplan, P.; DiMauro, S. Association of mutations in SCO2, a cytochrome c oxidase assembly gene, with early fetal lethality. *Arch. Neurol.* **2004**, *61* (6), 950−952.

(33) Cobine, P. A.; Pierrel, F.; Leary, S. C.; Sasarman, F.; Horng, Y. C.; Shoubridge, E. A.; Winge, D. R. The P174L mutation in human Sco1 severely compromises Cox17-dependent metallation but does not impair copper binding. *J. Biol. Chem.* **2006**, *281* (18), 12270−12276.
(34) Banting, G. S.; Glerum, D. M. Mutational analysis of the Saccharomyces cerevisiae cytochrome c oxidase assembly protein Cox11p. *Eukaryotic Cell* **2006**, *5* (3), 568−578.
(35) Smith, G. R.; Sternberg, M. J. E.; Bates, P. A. The relationship between the flexibility of proteins and their conformational states on forming protein-protein complexes with an application to protein-protein docking. *J. Mol. Biol.* **2005**, *347* (5), 1077−1101.
(36) Grunberg, R.; Leckner, J.; Nilges, M. Complementarity of structure ensembles in protein-protein binding. *Structure* **2004**, *12* (12), 2125−2136.
(37) Dominguez, C.; Bonvin, A. M. J. J.; Winkler, G. S.; van Schaik, F. M. A.; Timmers, H. T. M.; Boelens, R. Structural model of the UbcH5B/CNOT4 complex revealed by combining NMR, mutagenesis, and docking approaches. *Structure* **2004**, *12* (4), 633−644.
(38) van Dijk, A. D. J.; de Vries, S. J.; Dominguez, C.; Chen, H.; Zhou, H. X.; Bonvin, A. M. J. J. Data-driven docking: HADDOCK's adventures in CAPRI. *Proteins: Struct., Funct., Bioinf.* **2005**, *60* (2), 232−238.
(39) Smith, G. R.; Fitzjohn, P. W.; Page, C. S.; Bates, P. A. Incorporation of flexibility into rigid-body docking: Applications in rounds 3−5 of CAPRI. *Proteins: Struct., Funct., Bioinf.* **2005**, *60* (2), 263−268.
(40) Camacho, C. J. Modeling side-chains using molecular dynamics improve recognition of binding region in CAPRI targets. *Proteins: Struct., Funct., Bioinf.* **2005**, *60* (2), 245−251.
(41) Sali, A.; Blundell, T. L. Comparative protein modeling by satisfaction of spatial restraints. *J. Mol. Biol.* **1993**, *234* (3), 779−815.
(42) Vriend, G. What If—a molecularmodeling and drug design program. *J. Mol. Graphics* **1990**, *8* (1), 52−6.
(43) Altschul, S. F.; Madden, T. L.; Schaffer, A. A.; Zhang, J. H.; Zhang, Z.; Miller, W.; Lipman, D. J. Gapped BLAST and PSI-BLAST: a new generation of protein database search programs. *Nucleic Acids Res.* **1997**, *25* (17), 3389−3402.
(44) Banci, L.; Bertini, I.; Ciofi-Baffoni, S.; Katsari, E.; Katsaros, N.; Kubicek, K.; Mangani, S. A copper(I) protein possibly involved in the assembly of Cu-A center of bacterial cytochrome c oxidase. *Proc. Natl. Acad. Sci. U.S.A.* **2005**, *102* (11), 3994−3999.
(45) Thompson, J. D.; Higgins, D. G.; Gibson, T. J. Clustal-w—improving the sensitivity of progressive multiple sequence alignment through sequence weighting position-specific gap penalties and weight matrix choice. *Nucleic Acids Res.* **1994**, *22* (22), 4673−4680.
(46) Bradford, J. R.; Westhead, D. R. Improved prediction of protein-protein binding sites using a support vector machines approach. *Bioinformatics* **2005**, *21* (8), 1487−1494.
(47) Jorgensen, W. L.; Tirado-Rives, J. The OPLS Potential functions for proteins. Energy minimizations for crystals of cyclin peptides and crambin. *J. Am. Chem. Soc.* **1988**, *110* (6), 1657−1666.
(48) Kabsch, W.; Sander, C. Dictionary of protein secondary structure: pattern recognition of hydrogen-bonded and geometrical features. *Biopolymers* **1983**, *22* (12), 2577−2637.
(49) Nilges, M. A calculation strategy for the structure determination of symmetrical dimers by H-1-NMR. *Proteins: Struct., Func., Genet.* **1993**, *17* (3), 297−309.
(50) van Dijk, A. D. J.; Kaptein, R.; Boelens, R.; Bonvin, A. M. J. J. Combining NMR relaxation with chemical shift perturbation data to drive protein-protein docking. *J. Biomol. NMR* **2006**, *34* (4), 237−244.
(51) Zhou, H. Y.; Zhou, Y. Q. Distance-scaled, finite ideal-gas reference state improves structure-derived potentials of mean force for structure selection and stability prediction. *Protein Sci.* **2002**, *11* (11), 2714−2726.
(52) Camacho, C. J.; Zhang, C. FastContact: rapid estimate of contact and binding free energies. *Bioinformatics* **2005**, *21* (10), 2534−2536.
(53) Word, J. M.; Lovell, S. C.; LaBean, T. H.; Taylor, H. C.; Zalis, M. E.; Presley, B. K.; Richardson, J. S.; Richardson, D. C. Visualizing and quantifying molecular goodness-of-fit: Small-probe, contact dots with explicit hydrogen atoms. *J. Mol. Biol.* **1999**, *285* (4), 1711−1733.
(54) Davis, I. W.; Murray, L. W.; Richardson, J. S.; Richardson, D. C. MolProbity: structure validation and all-atom contact analysis for nucleic acids and their complexes. *Nucleic Acids Res.* **2004**, *32*, W615−W619.
(55) Wallace, A. C.; Laskowski, R. A.; Thornton, J. M. Ligplot—a program to generate schematic diagrams of protein ligand interactions. *Protein Eng.* **1995**, *8* (2), 127−134.
(56) Kraulis, P. J. MOLSCRIPT: A program to produce both detailled and schematic plots of protein structures. *J. Appl. Crystallogr.* **1991**, *24*, 946−950.
(57) Merrit, E. A.; Murphy, M. E. P. Raster3D version 2.0: A program for photorealistic molecular graphics. *Acta Crystallogr.* **1994**, *D50,* 869−873.

PR060651F